

states appear naturally at the onset of superconductivity, consistent with our experiment. On the basis of these symmetry arguments we conclude that the present experiment provides strong evidence for Cooper pairing with spin-triplet (*p*-wave) symmetry: a superconducting analogue of the A or A₁ phases of superfluid ³He. The distinction between unitary and non-unitary states in Sr₂RuO₄, however, cannot be made with the present results, and has to wait for further studies by other means. □

Received 27 March; accepted 30 June 1998.

1. Bardeen, J., Cooper, L. N. & Schrieffer, J. R. Theory of superconductivity. *Phys. Rev.* **108**, 1175–1204 (1957).
2. Sigrist, M. & Ueda, K. Phenomenological theory of unconventional superconductivity. *Rev. Mod. Phys.* **63**, 239–311 (1991).
3. Lee, D. M. The extraordinary phases of liquid ³He. *Rev. Mod. Phys.* **69**, 645–665 (1997).
4. Osheroff, D. D. Superfluidity in ³He: discovery and understanding. *Rev. Mod. Phys.* **69**, 667–681 (1997).
5. Richardson, R. C. The Pomeranchuk effect. *Rev. Mod. Phys.* **69**, 683–690 (1997).
6. Randall, J. J. & Ward, R. J. The preparation of some ternary oxides of the platinum metals. *J. Am. Chem. Soc.* **81**, 2629–2631 (1959).
7. Maeno, Y. *et al.* Superconductivity in a layered perovskite without copper. *Nature* **372**, 532–534 (1994).
8. Mackenzie, A. P. *et al.* Extremely strong dependence of superconductivity on disorder in Sr₂RuO₄. *Phys. Rev. Lett.* **80**, 161–164 (1998).
9. Mackenzie, A. P. *et al.* Quantum oscillations in the layered perovskite superconductor Sr₂RuO₄. *Phys. Rev. Lett.* **76**, 3786–3789 (1996).
10. Vollhardt, D. & Wölfle, P. *The Superfluid Phases of Helium 3* (Taylor & Francis, London, 1990).
11. Rice, T. M. & Sigrist, M. Sr₂RuO₄: an electronic analogue of ³He? *J. Phys. Condens. Matter* **7**, 643–648 (1995).
12. Baskaran, G. Why is Sr₂RuO₄ not a high T_c superconductor? Electron correlation, Hund's coupling and *p*-wave instability. *Physica B* **223 & 224**, 490–495 (1996).
13. Nishizaki, S., Maeno, Y., Farner, S., Ikeda, S. & Fujita, T. Pairing symmetry of superconducting Sr₂RuO₄ from specific heat measurements. *Physica C* **282–287**, 1413–1414 (1997).
14. Ishida, K. *et al.* Anisotropic pairing in superconducting Sr₂RuO₄: Ru NMR and NQR studies. *Phys. Rev. B* **56**, R505–R508 (1997).
15. Sigrist, M. & Zhitomirsky, M. E. Pairing symmetry of the superconductor Sr₂RuO₄. *J. Phys. Soc. Jpn* **65**, 3452–3455 (1996).
16. Machida, K., Ozaki, M. & Ohmi, T. Odd-parity pairing superconductivity under tetragonal symmetry—possible application to Sr₂RuO₄. *J. Phys. Soc. Jpn* **65**, 3720–3723 (1996).
17. Agterberg, D. F., Rice, T. M. & Sigrist, M. Orbital dependent superconductivity in Sr₂RuO₄. *Phys. Rev. Lett.* **78**, 3374–3377 (1997).
18. Brewer, J. H. in *Encyclopedia of Applied Physics* Vol. 11 (ed. Trigg, G. L.) 23 (VCH, New York, 1994).
19. Kiefl, R. F. *et al.* Search for anomalous internal magnetic fields in high-T_c superconductors as evidence for broken time-reversal symmetry. *Phys. Rev. Lett.* **64**, 2082–2085 (1990).
20. Luke, G. M. *et al.* Muon spin relaxation in UPT₃. *Phys. Rev. Lett.* **71**, 1466–1469 (1993).
21. Heffner, R. H. *et al.* New phase diagram for (U,TH)Be₁₃: a muon-spin-resonance and H_{1c1} study. *Phys. Rev. Lett.* **65**, 2816–2819 (1990).
22. Heffner, R. H. & Norman, M. R. Heavy fermion superconductivity. *Comments Condens. Matter Phys.* **17**, 361–408 (1996).
23. Uemura, Y. J., Yamazaki, T., Harshman, D. R., Senba, M. & Ansaldo, E. J. Muon-spin relaxation in AuFe and CuMn spin glasses. *Phys. Rev. B* **31**, 546–563 (1985).

Acknowledgements. We thank K. Machida, D. Agterberg and E. M. Forgan for discussions. Research at Columbia was supported by NSF and NEDO. Y.M. and Z.Q.M. thank CREST of the Japan Science and Technology Corporation for its support.

Correspondence and requests for materials should be addressed to G.M.L. (e-mail: luke@phys.columbia.edu).

Weekly cycles of air pollutants, precipitation and tropical cyclones in the coastal NW Atlantic region

Randall S. Cerveny & Robert C. Balling Jr

Office of Climatology and Department of Geography, Arizona State University, Tempe, Arizona 85287-1508, USA

Direct human influences on climate have been detected at local scales, such as urban temperature increases and precipitation enhancement^{1–3}, and at global scales^{4,5}. A possible indication of an anthropogenic effect on regional climate is by identification of equivalent weekly cycles in climate and pollution variables. Weekly cycles have been observed in both global surface temperature⁶ and local pollution⁷ data sets. Here we describe

statistical analyses that reveal weekly cycles in three independent regional-scale coastal Atlantic data sets: lower-troposphere pollution, precipitation and tropical cyclones. Three atmospheric monitoring stations record minimum concentrations of ozone and carbon monoxide early in the week, while highest concentrations are observed later in the week. This air-pollution cycle corresponds to observed weekly variability in regional rainfall and tropical cyclones. Specifically, satellite-based precipitation estimates indicate that near-coastal ocean areas receive significantly more precipitation at weekends than on weekdays. Near-coastal tropical cyclones have, on average, significantly weaker surface winds, higher surface pressure and higher frequency at weekends. Although our statistical findings limit the identification of cause–effect relationships, we advance the hypothesis that the thermal influence of pollution-derived aerosols on storms may drive these weekly climate cycles.

High concentrations of anthropogenic aerosols have been identified over the North Atlantic Ocean^{8–10}: a substantial amount of these pollutants are advected from the urbanized eastern seaboard of North America^{8,11}. We note that urban centres have a strong weekly pollution cycle^{7,12}. This variability, nicknamed the “Sunday effect”⁷, is characterized by high late-week pollution levels as opposed to the early week¹³ and, although still debated, is probably the result of car driving¹³. United States and Canadian inventories confirm higher weekday emissions as opposed to those of the weekend¹⁴.

If east-coast metropolitan areas display weekly pollution cycles and advection of that pollution is occurring, corresponding pollution cycles should be evident at downwind monitoring stations. To test this hypothesis, we used a 965-day (July 1991–January 1995) air-quality data set for Sable island (Fig. 1) as an indicator of pollution transport into the North Atlantic Ocean⁸. Concentrations (in p.p.b.v.) of two pollutants were monitored: ozone (O₃) and carbon monoxide (CO; a tracer for anthropogenic pollution¹⁵).

Because certain statistical techniques require a normal distribution, all data were tested for significant deviations from normality by computing standardized skewness and kurtosis coefficients^{16,17}. Atlantic pollution data sets met without transformation our significance criterion of $\alpha = 0.05$ which is used for all tests in this study. Barlett's test of variance dispersion reveals no significant difference in variance by day of the week. Displayed analysis is limited to data from April to October; research indicates that this period is most associated with ozone advection for the northern North Atlantic⁸. Recognizing that some data may have significant autocorrelation, we removed first-order autocorrelation from all data and found insignificant effects on our results. First-order autocorrelation results were also not significantly influenced by the few intermittent runs of zeroes in the precipitation dataset. We also adjusted the sample size for each analysis to reflect the potential influence of first-order autocorrelation, and again found no fundamental change in our results.

A seven-day cycle is evident in both O₃ and CO time series, with the late week (Thursday–Friday) experiencing highest values of pollutants and with lowest values associated with the early week (Sunday–Tuesday). After the two pollutants were standardized and combined into a single variable (Fig. 2a), a series of statistical analyses confirm weekly cyclicity in the CO + O₃ variable. First, a Student's *t*-test indicated a significant difference in daily mean concentrations between Monday and Thursday. Additional testing (with $\alpha = 0.0024$) using the assumption of completely independent daily data (to avoid the problem of multiplicity) still confirms the significant difference between the two extremes of the week. Second, spectral analysis identifies peaks in spectral density at seven days in CO, O₃ and CO + O₃ concentrations. Third, when the pollution data are categorized into 127 weekly periods, a 7-day sine wave (first harmonic) explains an average 50% of the variance in each weekly period. Fourth, shorter (~61 days, July–September 1991) data sets for Canadian Coast Guard lighthouses at Seal island, Nova Scotia

and Cape Race, Newfoundland⁸, as well as Sable island, also indicate significant differences in CO and O₃ between early- and late-week observations. Fifth, an independent pollution data set⁸ for Bermuda (where, owing to circulation, North American pollution advection creates early spring maxima in CO and O₃; ref. 11) shows a similar, but out of phase, weekly cycle in March and April with a mid-week pollution maximum. This phase shift in pollution transport between Sable island and Bermuda may result from changes in seasonal circulation strength and location.

Weekly cycles are associated with human activities rather than with natural phenomena⁶. No meteorological mechanism has a consistent seven-day return period. Consequently, identification of seven-day cycles in climate variables, coupled with the pollution cycle above, suggests direct anthropogenic forcing of regional climate. Investigation of such linkages is not new; examination of corresponding weekly cycles in rainfall and pollution date back to 1929¹⁹. For the present investigation, two independent climate data bases are examined. The first is a satellite record of daily precipitation over the world's oceans²⁰.

Daily oceanic precipitation values are available from Microwave Sounding Unit (MSU) channels 1, 2 and 3 as gathered by seven separate TIROS-N satellites²⁰ for 1 January 1979 to 31 March 1995. For this study, data were analysed for all oceanic 2.5° × 2.5° gridcells from 20° N to 60° N. An aggregate subset of 12 grid-cells was selected between 27.5° N and 42.5° N and within 5° longitude of the North American coast (Fig. 1) to isolate potential effects of eastern-seaboard pollution on oceanic precipitation. A fourth-root transformation of that data set produced the required gaussian distribution although our choice of transformation did not significantly affect our fundamental results. Aggregation removed potential spatial dependency problems²¹, and no difference in variance as a function of day was apparent.

For the hemispheric oceanic data set averaged over the 17-year time period, any given day comprises ~14.3% (one-seventh) of the weekly total. However, the aggregated near-coastal grid-cells show a distinctive intra-weekly variability. The greatest precipitation for these near-coastal grid-cells occur on Saturdays (658 mm yr⁻¹, 16.0%) while Mondays receive only 538 mm yr⁻¹ (13.1%) (Fig. 2b). Consequently, Saturday precipitation averages 22% higher than Monday precipitation.

Statistical tests confirm these findings. First, a one-tailed *t*-test indicates that the difference in means between Monday and Saturday is significant. Second, when the satellite rainfall estimates are

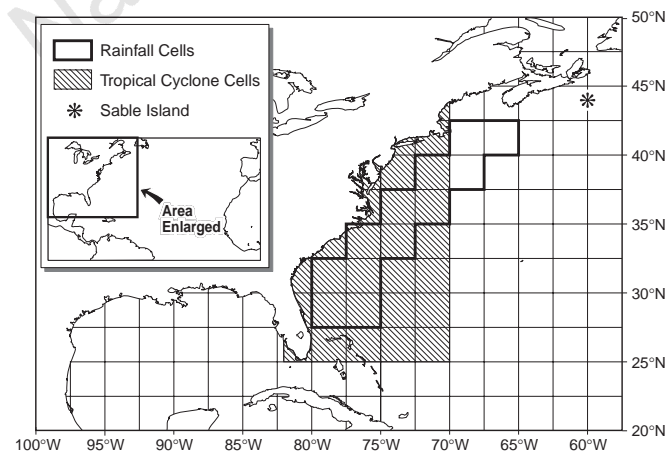


Figure 1 Location map. In the main figure, an asterisk shows the position of Sable island, monitoring site for CO and O₃ data; also shown are the 12 oceanic satellite-derived rainfall grid-cells (heavy lines; within 5° of the North American coast and between 27.5° N and 42.5° N) and the 'coastal' region of tropical cyclone observations (hatching; north of 25° N, west of 75° W, east of 82° W). Inset shows the location of the study area.

categorized into 847 weekly periods, a 7-day sine wave (first harmonic) explains an average 40% of the variance in each weekly period. Third, spectral analysis confirms the existence of a seven-day periodicity.

Fourth, the weekly cycle is also apparent downwind (east) of these grid-cells. A set of grid-cells for the mid-Atlantic constructed as a 30° longitude offset from the near-coastal grid-cells shows a weekly cycle in total precipitation which is confirmed by spectral analysis. Fifth, harmonic analysis of the average value by day of the week for each 2.5° × 2.5° grid-cell from 20° N to 60° N in the Atlantic reveals a distinct phase shift. Maximum precipitation occurs near the weekend for coastal grid-cells, and progresses to midweek for the mid-Atlantic. Mid-Atlantic grid-cells have precipitation peaks occurring on Tuesdays (396.7 mm yr⁻¹; 14.9%) and precipitation minima occurring on Saturdays (361.9 mm yr⁻¹; 13.6%). This pattern is consistent with eastward transport of pollution plumes^{8,11}.

A second independent test involves tropical cyclone analysis. Tropical cyclone data are derived from Atlantic observations (geographical positions, maximum wind strength, and minimum central pressure at six-hour intervals; 1886 to 1996) collected by the National Hurricane Center²². All observations are categorized by day of the week. Because of more limited hurricane data before 1946, only data from 1946 to 1996 are used.

An overestimation bias in reported winds exists between 1944 and 1969²³. Observations for that period are stronger by 4.9 m s⁻¹ than observations between 1970 and 1996. Although the segregation by day mitigates the overestimation, two separate analyses were

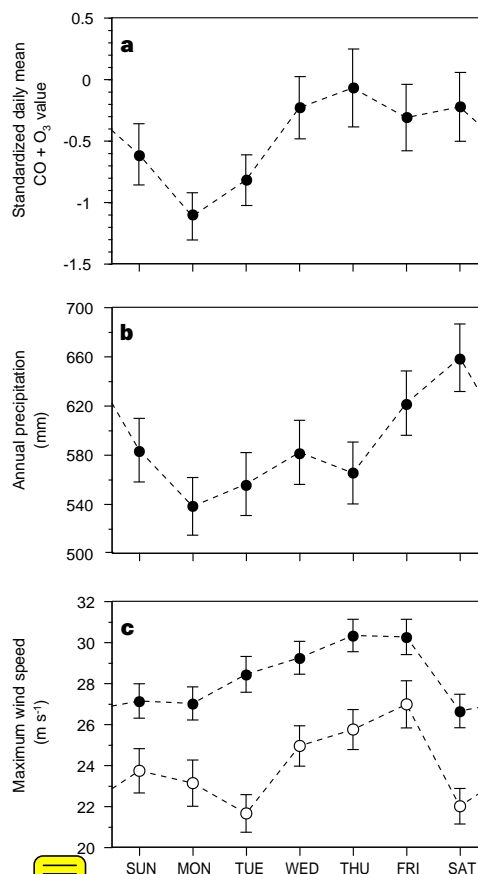


Figure 2 Mean values of three variables by day of the week; error bars show standard error of the mean ($\pm 1\sigma$). **a**, Mean values for the summed composite of the standardized species (CO and O₃) for Sable island, 1991–95 (the mean of the composite is nonzero owing to the exclusion of missing data pairs); **b**, total annual precipitation for grid-cells identified in Fig. 1; and **c**, tropical cyclonic mean maximum wind speed for the 'long' (filled circles) data set (1946–96) and 'short' (open circles) data set (1970–96).

conducted to fully compensate for this bias. The first analysis used the entire database ('long') while the second used only the unbiased (1970–96) observations ('short'). The total database showed no significant differences by day of the week in observation frequency, maximum surface wind speeds, or minimum central pressure. All tropical cyclone data sets met normality criteria.

Two regions are defined; 'coastal' incorporates all tropical cyclone observations north of 25° N, west of 70° W but east of 82° W (Fig. 1) and 'non-coastal' includes all tropical cyclone observations outside the 'coastal' parameters. As with the total data set, the 'non-coastal' data set shows no significant variation in strength or frequency by day of the week. For the 'non-coastal' data set, neither minimum central pressure nor maximum surface wind show weekly variability. Additionally, no differences exist in observation frequency by day of the week for the 'non-coastal' data set.

Conversely, the 'coastal' tropical cyclone data set shows an explicit weekly cycle (Fig. 2c). Both 'long' and 'short' 'coastal' weekend observations significantly vary from mid-week observations. For the 'long' data set, maximum surface winds average 5.0 m s⁻¹ slower for observations made on Saturdays than those for Fridays (Fig. 2c). The unbiased 'short' data set has Saturday wind observations averaging 3.6 m s⁻¹ slower than those on Friday; these differences are highly significant.

Significant differences are also apparent in minimum central pressures (not shown). The 'short' data set's Saturday observations average 6.3 hPa higher in central minimum pressure than for Thursday. Because of the discontinuous nature of the tropical cyclone data, spectral analysis is not applicable. However, when the maximum wind data are categorized into 396 separate weekly periods, a 7-day sine wave (first harmonic) explains an average 55% of the variance in each weekly period.

Because our goal is to emphasize the long-term existence, not direct comparison, of weekly cycles in three independent variables, caution is urged in applying day-to-day correspondences between the three weekly cycles. However, proving the existence of equivalent cycles is a time-honoured scientific methodology; for example, research linking cycles in palaeoclimate reconstructions with equivalent astronomical cycles²⁴. Cycle identification is particularly important if a physical rationale can be advanced to explain cyclic similarities.

Theories proposed in hurricane modification studies²⁵ and urban climate modification studies^{3,26–28} may explain the similar cycles in climate and pollution. Heavy aerosol loading can produce thermal responses in storm intensity and precipitation development^{2,25,29,30} such that modification of the boundary layer's thermal structure leads to increased turbulence and enhanced precipitation^{29,30}, and that solar radiation absorption by massive aerosol loading around a hurricane cloud cluster stimulates cumulus convection²⁵. We propose that extensive regional pollution advection into the Atlantic produces climate modification by these mechanisms. As our findings are statistical in nature, we can not confirm such a cause-and-effect hypothesis, but we propose this hypothesis to stimulate research on potential causative mechanisms operating between pollution and regional climate. □

Received 30 December 1996; accepted 20 May 1998.

1. Changnon, S. A. Jr METROMEX: A review and summary. *Meteorol. Monogr.* **40**, 1–181 (1981).
2. Dettwiler, J. W. & Changnon, S. A. Jr Possible urban effects on maximum daily rainfall at Paris, St. Louis and Chicago. *J. Appl. Meteorol.* **15**, 517–519 (1976).
3. Ackerman, B. S. *et al.* Summary of METROMEX Vol. 2, Causes of Precipitation Anomalies (Illinois State Water Survey, Urbana, IL, 1978).
4. Houghton, J. T. *et al.* (eds) *Climate Change 1995: The Science of Climate Change* (Cambridge Univ. Press, 1996).
5. Tett, S. F. B., Mitchell, J. F. B., Parker, D. E. & Allen, M. R. Human influence on the atmosphere vertical temperature structure: Detection and observations. *Science* **274**, 1170–1173 (1996).
6. Gordon, A. H. Weekdays warmer than weekends? *Nature* **367**, 325–326 (1994).
7. Graedel, T. E., Farrow, L. A. & Weber, T. A. Photochemistry of the 'Sunday Effect'. *Environ. Sci. Technol.* **11**, 690–694 (1977).
8. Parrish, D. D. *et al.* Export of North American ozone pollution to the North Atlantic Ocean. *Science* **259**, 1436–1439 (1993).
9. Pueschel, R. J., Boatman, J. F. & Artz, R. S. Aerosols over the western Atlantic: Scale heights, concentrations, and fluxes. *Atmos. Environ.* **22**, 2371–2380 (1988).
10. Anderson, B. E. *et al.* The impact of U.S. continental outflow on ozone and aerosol distributions over

- the Western Atlantic. *J. Geophys. Res.* **98**(D12), 23477–23489 (1993).
11. Dickerson, R. R., Doddridge, B. G. & Kelley, P. Large-scale pollution of the atmosphere over remote Atlantic Ocean: Evidence from Bermuda. *J. Geophys. Res.* **100**, 8945–8952 (1995).
12. Cleveland, W. S., Graedel, T. E., Kleiner, B. & Warner, J. L. Sunday and workday variations in photochemical air pollutants in New Jersey and New York. *Science* **186**, 1037–1038 (1974).
13. Siegel, S. L., Arcado, T. D. & Lawson, D. R. Weekday vs. weekend ambient ozone concentration: Discussion and hypotheses with focus on Northern California. *Journal of Air and Waste Management Association* **45**, 967–972 (1995).
14. Saeger, M. *et al.* *The 1985 NAPAP Emissions Inventory (Version 2): Development of the Annual Data and Modelers' Tapes* (US Environmental Protection Agency, Washington DC, 1989).
15. Fishman, J. & Seiler, W. Correlative nature of ozone and carbon monoxide in the troposphere: Implications for the tropospheric ozone budget. *J. Geophys. Res.* **88**, 3662 (1983).
16. Keeping, E. S. *Introduction to Statistical Inference* (Van Nostrand, Princeton, NJ, 1962).
17. Siegel, S. *Non-Parametric Statistics* (McGraw-Hill, New York, 1956).
18. Oltmans, S. J. & Levy, I. H. Seasonal cycle of surface ozone over the western North Atlantic. *Nature* **358**, 392–394 (1992).
19. Ashworth, J. R. The influence of smoke and hot gases from factory chimneys on rainfall. *Q. J. R. Meteorol. Soc.* **55**, 841–850 (1929).
20. Spencer, R. W. Global oceanic precipitation from the MSU during 1979–1991 and comparisons with other climatologies. *J. Clim.* **6**, 1301–1326 (1993).
21. Livezey, R. E. & Chen, W. Y. Statistical field significance and its determination by Monte Carlo techniques. *Mon. Weath. Rev.* **111**, 46–59 (1983).
22. Jarvinen, B. R., Neumann, C. J. & Davis, M. A. S. *A Tropical Cyclone Data Tape for the North Atlantic Basin, 1886–1983: Contents, Limitations, and Uses* (US Dept of Commerce, NOAA, Weather Service, Natl Hurricane Center, Coral Gables, Florida, 1984).
23. Landsea, C. W. A climatology of intense (or major) Atlantic hurricanes. *Mon. Weath. Rev.* **121**, 1703–1713 (1993).
24. Hays, J. D., Imbrie, J. & Shackleton, N. J. Variations in the earth's orbit: Pacemaker to the ice ages. *Science* **194**, 1121–1132 (1976).
25. Gray, W. M., Frank, W. M., Corrin, M. L. & Stokes, C. A. Weather modification by carbon dust absorption of solar energy. *J. Appl. Meteorol.* **15**, 355–386 (1976).
26. Gallo, K. P., Tarpley, J. D., McNab, A. L. & Karl, T. R. Assessment of urban heat islands: A satellite perspective. *Atmos. Res.* **37**, 37–43 (1995).
27. Oke, T. R., Johnson, G. T., Steyn, D. G. & Watson, I. D. Simulation of surface urban heat islands under 'ideal' conditions at night, Part 2: diagnosis of causation. *Bound. Lay. Meteorol.* **36**, 339–358 (1991).
28. Henry, J. A., Dicks, S. E., Wetterquist, O. F. & Roguski, S. J. Comparison of satellite, ground-based, and modeling techniques for analyzing the urban heat island. *Photogr. Eng. Remote Sensing* **55**, 69–76 (1989).
29. Atkinson, B. W. The effect of an urban area on the precipitation from a moving thunderstorm. *J. Appl. Meteorol.* **10**, 47–55 (1971).
30. Changnon, S. A. Jr Recent studies of urban effects on precipitation in the United States. *Bull. Am. Meteorol. Soc.* **50**, 411–421 (1969).

Acknowledgements. We thank D. Parrish for the Canadian pollution data, S. J. Oltmans for the Bermuda ozone data, C. Landsea for the tropical cyclone database, and R. Spencer for the MSU daily precipitation data set.

Correspondence and requests for materials should be addressed to R.S.C. (e-mail: cerveny@asu.edu).

Stable phytoplankton community structure in the Arabian Sea over the past 200,000 years

C. J. Schubert*†, J. Villanueva*†, S. E. Calvert*, G. L. Cowie*†, U. von Rad‡, H. Schulz‡, U. Berner‡ & H. Erlenkeuser§

* Department of Earth and Ocean Sciences, University of British Columbia, Vancouver, British Columbia, Canada V6T 1Z4

‡ Bundesanstalt für Geowissenschaften und Rohstoffe, D-30631 Hannover, Germany

§ Leibniz-Labor für Altersbestimmung und Isotopenforschung, Universität Kiel, D-24118 Kiel, Germany

Glacial to interglacial climate changes have been related to organic carbon cycling in oceanic surface waters¹, and this possible link has led to the development of sedimentary tracers of past marine biological production. For example, sediment records of organic carbon², opal³ and biogenic barium⁴ have been used to reconstruct past variations in production in different oceanic regimes, but these tracers cannot be used to discriminate between the relative contributions of different phytoplankton groups. Such a discrimination would provide greater insight into

† Present addresses: Max Planck Institute for Marine Microbiology, Celsiusstrasse 1, 28359 Bremen, Germany (C.J.S.); Département de Géologie et Océanographie, UMR CNRS 5805, Université de Bordeaux I, Avenue des Facultés, 33405 Talence Cedex, France (J.V.); Geology and Geophysics Department, University of Edinburgh, Edinburgh EH9 3JW, UK (G.L.C.).